



## Potential microbial mechanisms driving granular activated carbon-enhanced syntrophic propionate degradation under elevated organic loading rates

Title	Potential microbial mechanisms driving granular activated carbon-enhanced syntrophic propionate degradation under elevated organic loading rates
Author(s)	Liu, Tingxia;Liu, Chuanqi;Chang, Huanhuan;Wu, Qianyuan;Wang, Wenlong;Wu, Guangxue
Publication Date	2026-01-21
Publisher	Elsevier
Repository DOI	<a href="https://doi.org/10.1016/j.jece.2026.121343">https://doi.org/10.1016/j.jece.2026.121343</a>



# Potential microbial mechanisms driving granular activated carbon-enhanced syntrophic propionate degradation under elevated organic loading rates

Tingxia Liu <sup>a, b</sup>, Chuanqi Liu <sup>b</sup>, Huanhuan Chang <sup>a</sup>, Qianyuan Wu <sup>c</sup>, Wenlong Wang <sup>c</sup>, Guangxue Wu <sup>a, \*</sup>

<sup>a</sup> Civil Engineering, School of Engineering, College of Science and Engineering, University of Galway, Galway H91 TK33, Ireland

<sup>b</sup> College of Environmental Science and Engineering, Beijing Forestry University, Beijing 100083, China

<sup>c</sup> Shenzhen Key Laboratory of Ecological Remediation and Carbon Sequestration, Environmental Protection Key Laboratory of Microorganism Application and Risk Control, Institute of Environment and Ecology, Shenzhen International Graduate School, Tsinghua University, Shenzhen 518055, China

## ARTICLE INFO

### Keywords:

Anaerobic digestion  
Granular activated carbon  
Microbial adaptation  
Oxidative stress  
Propionate degradation

## ABSTRACT

Anaerobic digestion is a sustainable technology for organic wastes treatment and energy recovery. However, propionate accumulation under environmental stress disrupts microbial balance, resulting in reduced methane yield and system instability. In this study, the effect of granular activated carbon (GAC) on propionate degradation under high organic loading rates (OLRs) was investigated. In the long-term operation, the GAC-amended reactor enhanced methane yield and propionate removal efficiency by 7.4 % and 11.6 %, respectively, at an OLR of 7 g chemical oxygen demand/L/d. Short-term GAC addition showed a stronger effect in sludge from the GAC-amended reactor, with 16.2–34.1 % increases in propionate degradation rates and 27.0–33.9 % enhancements in maximum methane production rates compared with the sludge from the reactor without GAC addition under N<sub>2</sub> or high hydrogen partial pressure. Additionally, GAC maintained a high microbial diversity under high-OLR conditions and enriched *Smithella* and *Mesotoga*. GAC could facilitate propionate conversion via key metabolic pathways, including propionate oxidation and syntrophic acetate oxidation. Furthermore, GAC may alleviate oxidative stress and enhance bacterial membrane resilience, increasing microbial resistance to high OLR stress. Genes associated with extracellular electron transfer were increased by 14.3–65.8 % in the presence of GAC. Collectively, GAC enhanced methanogenic propionate degradation and overall system stability. This study highlights GAC-driven microbial adaptations under environmental stress and provides guidance for applying conductive materials to optimize high-loading anaerobic reactors.

## 1. Introduction

Anaerobic digestion (AD) is a mature, environmentally sustainable biotechnology, which is widely applied for stabilizing organic waste while recovering methane as a renewable bioenergy. However, in practical operation, fluctuations in organic loading often challenge system stability, leading to volatile fatty acids (VFAs) accumulation, particularly under elevated organic loading rates (OLRs) [1]. Previous studies have highlighted the adverse effects of high organic loading on anaerobic system performance. For example, increasing the OLR to 10 g chemical oxygen demand (COD)/L/d has been reported to cause the accumulation of acetate and propionate during agro-industrial waste

treatment [2–4], with more accumulation likely at higher OLRs. VFAs accumulation typically results in pH decline, inhibition of microbial activity, and possible failure of the AD process [5]. Moreover, recent studies indicate that VFAs accumulation can induce oxidative stress by triggering excessive production of reactive oxygen species (ROS), further impairing microbial metabolic functions [6,7].

Among VFAs, propionate is particularly prone to accumulation due to the thermodynamic constraints of its degradation [8,9]. Such accumulation is closely associated with methanogenic inhibition, leading to decreased methane yield and system instability. For instance, a decrease in methane production efficiency has been observed in an anaerobic reactor with an accumulated propionate concentration of 2.8 g/L [10].

\* Corresponding author.

E-mail address: [guangxue.wu@universityofgalway.ie](mailto:guangxue.wu@universityofgalway.ie) (G. Wu).

<https://doi.org/10.1016/j.jece.2026.121343>

Received 14 November 2025; Received in revised form 9 January 2026; Accepted 19 January 2026

Available online 19 January 2026

2213-3437/© 2026 The Author(s). Published by Elsevier Ltd. This is an open access article under the CC BY license (<http://creativecommons.org/licenses/by/4.0/>).

Propionate concentrations of 6.5–14.6 mM have been reported to induce a lag phase and inhibit biogas production during anaerobic co-digestion of food waste and dairy manure [11]. Consequently, improving the efficiency of propionate degradation is critical for maintaining the stable performance of AD processes under high OLR stress conditions.

Conductive materials (CMs) have emerged as effective additives to enhance methane yield and stability of AD systems under environmental stress, including overloading, suboptimal alkalinity conditions, and inhibitory compounds [12–14]. Among them, granular activated carbon (GAC), characterized by its high surface area and strong conductivity, has been widely applied to reinforce microbial interactions and process stability [15,16]. For instance, GAC improved COD removal efficiency by 13.7 % and methane yield by 26.9 % in upflow anaerobic sludge blanket (UASB) reactors treating propionate-rich synthetic wastewater [17]. Moreover, He et al. [18] reported that GAC enabled stable operation of brewery wastewater UASBs even at an OLR of 17.5 g COD/L/d. These benefits of GAC could be associated with direct interspecies electron transfer (DIET), the enrichment of functional microbes, and increased abundance of genes coding for conductive pili, OmcS, and quorum sensing [13,19]. In addition, recent studies suggest that CMs, such as nano magnetite and Fe<sub>3</sub>O<sub>4</sub>, can alleviate propionate stress by upregulating genes in stress defense systems [20,21]. Despite these advances, the potential of GAC to mitigate propionate accumulation under high OLRs, as well as its effects on syntrophic interactions and microbial stress responses, has not been systematically investigated.

To address the above-mentioned knowledge gaps, this study evaluated the effects of GAC supplementation on methane yield and propionate removal with increasing OLRs. Subsequently, the effect of short-term GAC supplementation was investigated. Propionate degradation activity tests, together with targeted assays under high hydrogen partial pressure (HPP), were conducted to assess microbial acclimation and its physicochemical implications. Functional predictions using Phylogenetic Investigation of Communities by Reconstruction of Unobserved States (PICRUSt2) were also performed to examine potential changes in metabolic pathways, oxidative stress defense, membrane biosynthesis, and electron transfer in GAC-amended reactors under high loading conditions. Collectively, this study aims to provide multi-dimensional insights into the mechanisms underlying GAC-driven stabilization of syntrophic propionate degradation and to regulate AD performance under environmental stress.

## 2. Materials and methods

### 2.1. Reactor setup and inoculum

Two UASB reactors (working volume of 3.5 L) were operated at 35 ± 2°C for 88 days. Previous studies have examined the impact of propionate loading (0.5–30 g COD/L/d) on anaerobic reactor performance, where methanogenesis inhibition has been reported at thresholds of 4.5–23.0 g COD/L/d [9,22,23]. Based on these findings, stepwise propionate loadings of 4–7 g COD/L/d were applied in this study to evaluate the role of GAC in alleviating high OLR stress. The operation was divided into four phases, i.e., Phase I (days 1–25, 4 g COD/L/d), Phase II (days 26–39, 5 g COD/L/d), Phase III (days 40–54, 6 g COD/L/d), and Phase IV (days 55–88, 7 g COD/L/d). Granular sludge collected from a dairy wastewater treatment reactor was used as the inoculum, with suspended solids (SS) and volatile suspended solids (VSS) concentrations of 7.0 g/L and 5.6 g/L, respectively. One reactor was supplemented with 5 g/L GAC (20–40 mesh, Sigma-Aldrich, Ireland) only at the start-up stage and was referred to as UASB<sub>GAC</sub>, while the other without GAC served as the control reactor (UASB<sub>CON</sub>). The hydraulic retention time for both reactors was maintained at 12 h. No sludge was manually discharged during the operation.

Propionate was used as the sole organic carbon source, with a COD:N:P ratio of 200:5:1. Nitrogen and phosphorus were supplied by NH<sub>4</sub>Cl and Na<sub>2</sub>HPO<sub>4</sub>. Inorganic constituents of the synthetic medium included

500 mg/L KHCO<sub>3</sub>, 500 mg/L NaHCO<sub>3</sub>, 197 mg/L CaCl<sub>2</sub>·6 H<sub>2</sub>O, 250 mg/L MgSO<sub>4</sub>, and 1 mL/L trace element solution, as described by Du et al. [24].

### 2.2. Batch experiments

To further elucidate the promoting mechanisms of GAC on propionate degradation under environmental stress, two batch experiments were conducted at the end of Phase IV. One assessed the impact of short-term GAC supplementation, and the other evaluated its effect under high HPP.

For the first assay, four treatments were applied, i.e., sludges from the UASB<sub>CON</sub> and UASB<sub>GAC</sub> reactors (referred to as N<sub>2</sub>-CON and N<sub>2</sub>-GAC, respectively), and sludges supplemented with an additional 5 g/L GAC (referred to as N<sub>2</sub>-CON<sub>+GAC</sub> and N<sub>2</sub>-GAC<sub>+GAC</sub>, respectively). Anaerobic conditions were created by purging the bottles with N<sub>2</sub> for 3 min and sealed with butyl rubber stoppers.

For the second assay, the same conditions as the first assay were applied, while an additional high HPP (~0.42 atm) was established following Zhang et al. [25]. Briefly, after N<sub>2</sub> purging, H<sub>2</sub> was injected into the headspace to achieve approximately 25 mL of H<sub>2</sub> at 293 K. The four treatments were denoted as H<sub>2</sub>-CON, H<sub>2</sub>-CON<sub>+GAC</sub>, H<sub>2</sub>-GAC, and H<sub>2</sub>-GAC<sub>+GAC</sub>, respectively.

All assays were performed in 160 mL serum bottles with 100 mL working volume and 60 mL headspace. Sludge collected from the two UASB reactors was adjusted to a VSS concentration of 2 g/L, and propionate was supplemented at 1000 mg COD/L. All bottles were incubated at 35°C and 170 rpm under anaerobic conditions.

During experiment, headspace gas (100 µL) and liquid samples (0.5 mL) were periodically collected to determine methane production and VFAs concentrations. Propionate degradation rates were estimated by linear fitting. Methane production was calculated based on headspace pressure and methane content, as described by Wang et al. [26]. The modified Gompertz model [27] was used to fit methane production kinetics:

$$P = P_{\max} \exp \left\{ - \exp \left[ \frac{e R_{\max}}{P_{\max}} (\lambda - t) + 1 \right] \right\}$$

where  $P$  represents the CH<sub>4</sub> production volume (mL/L),  $P_{\max}$  is the potential maximum CH<sub>4</sub> production volume (mL/L),  $R_{\max}$  is the maximum CH<sub>4</sub> production rate (mL/L/h),  $e$  is the base of the natural logarithm ( $e = 2.71828$ ),  $\lambda$  is the CH<sub>4</sub> production lag phase (h), and  $t$  is the reaction time (h). All assays were performed in triplicate.

### 2.3. Analytical methods

SS and VSS concentrations were measured according to standard methods [28]. A high-performance liquid chromatography (HPLC, Agilent 1260, USA) with a UV detector was used to detect VFAs concentrations. An Aminex HPX-87H column was employed with 0.1 % H<sub>2</sub>SO<sub>4</sub> as the mobile phase. The injection volume was 30 µL, the column temperature was 55°C, and the flow rate was 0.8 mL/min. The gas chromatograph (7890 A, Agilent, Santa Clara, USA) equipped with a thermal conductivity detector was used to determine methane concentration. Additionally, the headspace pressure in the serum bottles was measured using a portable pressure gage (Testo 512, Testo, Titisee-Neustadt, Germany).

Welch's  $t$ -test was performed in Microsoft Excel to assess differences between group means. Pearson correlation and one-way analysis of variance (ANOVA) followed by Tukey's HSD post hoc tests were performed using SPSS version 26.0. In all analyses,  $p < 0.05$  was considered statistically significant. Methane production kinetics were analyzed, and data visualization was conducted using OriginPro 2021 (OriginLab, USA).

## 2.4. Microbial community and functional prediction analysis

Sludge samples were collected from both UASB<sub>CON</sub> and UASB<sub>GAC</sub> reactors at the end of each operational phase (Phases I–IV) to analyze microbial community composition and metabolic pathways. Samples were labeled as CON1 to CON4 and GAC1 to GAC4, corresponding to samples collected from UASB<sub>CON</sub> and UASB<sub>GAC</sub>, respectively. At each sampling point, total DNA was extracted from the sludge using the DNeasy PowerSoil Pro Kit (QIAGEN, UK) following the manufacturer's instructions. NanoDropOne (Thermo Fisher Scientific, USA) was used to detect the concentration of DNA. To analyze the microbial community structure, high throughput 16S rRNA gene sequencing was conducted. Polymerase chain reaction amplification was carried out with universal primers 515 F (5'-GTGCCAGCMGCCGCGGTAA-3') and 806 R (5'-GGACTACHVGGGTWTCTAAT-3') targeting the V4 region, covering both bacterial and archaeal 16S rRNA genes. The Illumina HiSeq 2500 platform (Illumina, San Diego, USA) was used for high-throughput sequencing. The obtained DNA sequences were subjected to quality trimming and assigned to operational taxonomic units (OTUs) with a 97 % similarity cut-off. The representative sequence of each OTU was aligned with the SILVA/v132 database (<https://www.arb-silva.de/>) to obtain the microbial community structure.

PICRUSt2 was applied to predict the relative abundance of functional genes and metabolic pathways [29]. Genes were annotated against the Kyoto Encyclopedia of Genes and Genomes (KEGG) database. Gene abundance values were row-wise Z-score standardized (mean-centered and scaled to unit variance) to enhance visualization. Relative abundances of enzymes are presented in Table S1. Alpha diversity indices and principal coordinates analysis (PCoA) were generated using the

Magigene Cloud Platform (<http://cloud.magigene.com/>), and PICRUSt2 analyses were performed on the Bioincloud platform (<https://www.bioincloud.tech/>).

## 3. Results and discussion

### 3.1. System response to stepwise increased OLRs

Both UASB<sub>CON</sub> and UASB<sub>GAC</sub> reactors exhibited improved methane yield with increasing OLRs. As shown in Fig. 1a, methane yield in the UASB<sub>GAC</sub> reactor increased steadily from 124.4 mL/g COD on Day 2 to 298.4 mL/g COD by Day 86, while the UASB<sub>CON</sub> reactor showed a slower increase, stabilizing at approximately 270 mL/g COD. The disconnected points in Fig. 1a were caused by gas collection bag leakage, resulting in no biogas measurements for those days. Importantly, methane yield in the UASB<sub>GAC</sub> reactor consistently exceeded that of the UASB<sub>CON</sub> reactor at the OLR of 7 g COD/L/d, with an average increase of 7.4 %, highlighting the enhanced methanogenic capacity associated with GAC addition. This observation aligns with previous studies that CMs can enhance methane yield by 6–125 % via facilitating interspecies electron transfer in AD systems [15,30–32].

This enhanced performance was corroborated by effluent propionate levels. While both reactors exhibited comparable removal during Phase I, effluent propionate concentrations in the UASB<sub>CON</sub> reactor gradually increased with increasing OLRs, reaching 500–700 mg COD/L by Phase IV. A similar trend was observed in static semi-continuous bioreactors, where a propionate loading of 3 g COD/L/d resulted in continuous propionate accumulation of about 10 g/L [33]. In contrast, the UASB<sub>GAC</sub> reactor maintained effective propionate degradation, with

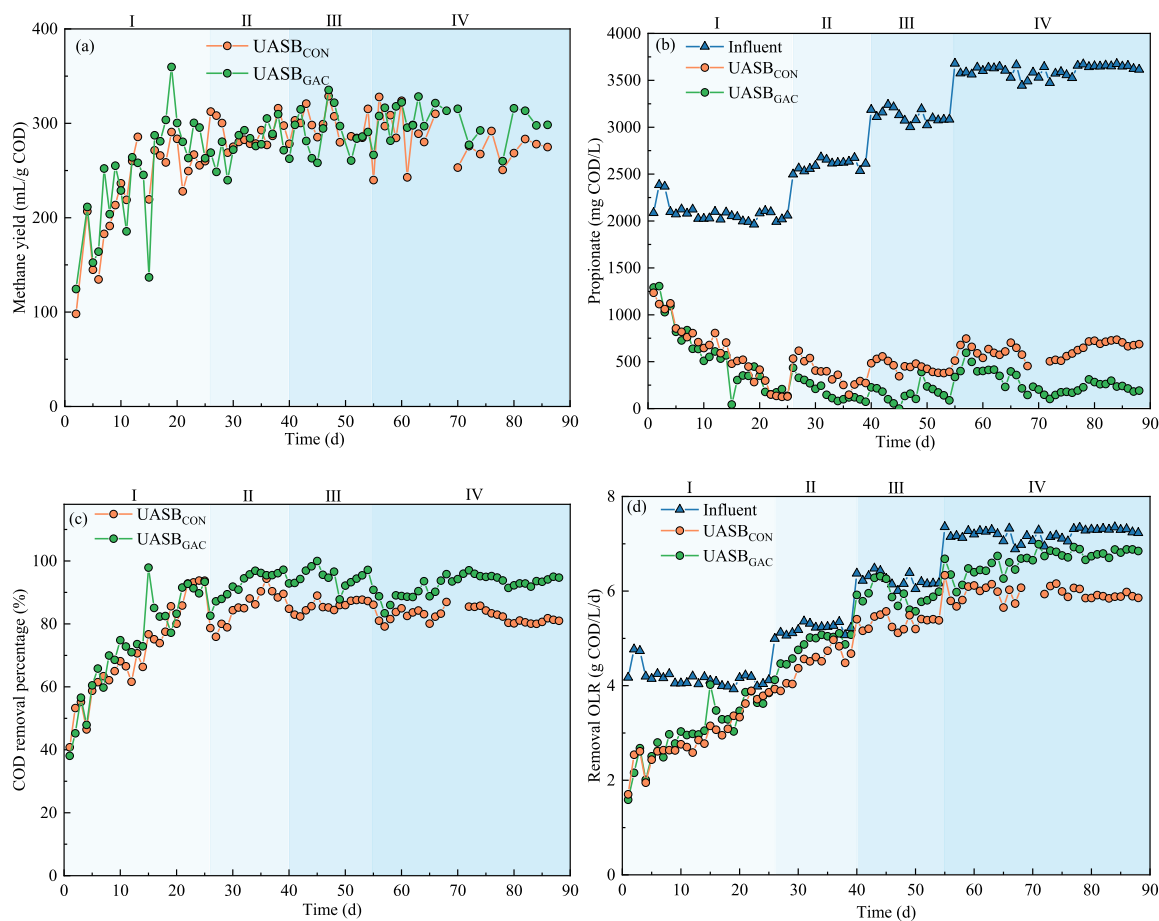


**Fig. 1.** Performance comparison of two UASB reactors during long-term operation: (a) Methane yield; (b) Influent and effluent propionate concentrations; (c) COD removal efficiency; (d) Organic loading removal capacity.

concentrations below 300 mg COD/L at Phase IV (Fig. 1b). Similarly, the UASB<sub>GAC</sub> reactor consistently achieved COD removal efficiencies exceeding 90 %, outperforming the UASB<sub>CON</sub> reactor, particularly under high OLR conditions (e.g.,  $94.6 \pm 0.4$  % vs.  $81.4 \pm 0.4$  % at Phase IV; Table 1). Moreover, the UASB<sub>GAC</sub> reactor exhibited a higher organic loading removal efficiency, particularly during Phase IV, where its removal capacity was 1.2-fold that of the UASB<sub>CON</sub> reactor (Fig. 1d). These observations indicate that the benefits of CMs in enhancing system performance are more pronounced under high OLR conditions, consistent with previous studies [34–36].

In summary, the UASB<sub>GAC</sub> reactor demonstrated superior long-term performance in both methane yield and propionate removal, particularly under elevated OLRs, highlighting GAC addition as an effective strategy to enhance reactor resilience and operational stability under high OLR stress. These enhancements may be associated with multiple interrelated mechanisms, such as syntrophic enrichment, accelerated DIET, and the upregulation of key functional genes, as suggested by previous studies [20,37,38]. To elucidate the potential stimulating mechanisms, this study next assessed microbial propionate degradation activity under short-term GAC supplementation and other microbial- and genomic-level responses.

### 3.2. Benefits and potential mechanistic insights of GAC on propionate degradation

#### 3.2.1. Short-term GAC effects on microbial activity under N<sub>2</sub>-purged conditions

As shown in Fig. 2, no significant difference was observed between the N<sub>2</sub>-CON group and N<sub>2</sub>-GAC group ( $p > 0.05$ ) in propionate degradation. This observation is consistent with the long-term reactor performance, where both reactors exhibited comparable degradation efficiencies under low OLRs. Additionally, short-term GAC supplementation had no significant effect on propionate degradation activity in sludge from the UASB<sub>CON</sub> reactor ( $p > 0.05$ ). In contrast, the N<sub>2</sub>-GAC<sub>+GAC</sub> group exhibited 21.8 % and 28.0 % higher propionate degradation rate and maximum methane production rate ( $R_{max}$ ), respectively, as well as a 31.3 % shorter lag phase relative to the N<sub>2</sub>-GAC group ( $p < 0.05$ ). Furthermore, compared with N<sub>2</sub>-CON<sub>+GAC</sub>, the N<sub>2</sub>-GAC<sub>+GAC</sub> group showed 34.1 % and 27.0 % higher degradation rate and  $R_{max}$ , respectively, and a 32.5 % shorter lag phase. Collectively, these findings indicate that while short-term GAC exposure alone is insufficient to stimulate unacclimated sludge, its benefits become evident in GAC-adapted biomass—emphasizing the critical role of pre-acclimated microbial consortia.

The superior performance of the N<sub>2</sub>-GAC<sub>+GAC</sub> group likely arose from a synergistic interplay between long-term microbial acclimation and short-term conductive surface effects. On one hand, long-term GAC exposure may have selectively enriched syntrophic microbial populations within the UASB<sub>GAC</sub> reactor, thereby promoting microbial adaptation [39]. On the other hand, this study hypothesized that the additional GAC provided conductive surfaces that may have facilitated DIET, which reinforced syntrophic associations and improved degradation efficiency [24].

**Table 1**

Long-term operational performance of UASB<sub>CON</sub> and UASB<sub>GAC</sub> reactors.

Parameters	Phase I (Day 1–25)		Phase II (Day 26–39)		Phase III (Day 40–54)		Phase IV (Day 55–88)	
	UASB <sub>CON</sub>	UASB <sub>GAC</sub>	UASB <sub>CON</sub>	UASB <sub>GAC</sub>	UASB <sub>CON</sub>	UASB <sub>GAC</sub>	UASB <sub>CON</sub>	UASB <sub>GAC</sub>
OLR (g COD/L/d)	4		5		6		7	
Influent COD (mg/L)	2023.3 ± 33.5		2606.8 ± 69.8		3079.3 ± 4.3		3630.6 ± 21.4	
Effluent COD (mg/L)	130.1 ± 5.2	172.3 ± 35.6	274.7 ± 18.3	97.2 ± 24.0	384.1 ± 7.2	133.7 ± 42.7	676.0 ± 11.0	195.8 ± 16.8
COD removal percentage (%)	93.6 ± 0.3	91.5 ± 1.8	89.4 ± 1.0	96.3 ± 0.9	87.5 ± 0.2	95.7 ± 1.4	81.4 ± 0.4	94.6 ± 0.4
Organic removal rate (g COD/L/d)	3.8 ± 0.1	3.7 ± 0.1	4.7 ± 0.2	5.0 ± 0.1	5.4 ± 0.0	5.9 ± 0.1	5.9 ± 0.1	6.9 ± 0.0
Recovery duration (d)	0	0	2	1	2	1	3	3

#### 3.2.2. GAC-facilitated propionate degradation under high HPP

As shown in Fig. 3b and d, the H<sub>2</sub>-GAC group exhibited slightly higher propionate degradation rates and  $R_{max}$  than the H<sub>2</sub>-CON group, although these differences were not statistically significant ( $p > 0.05$ ). However, a significant reduction in the lag phase was observed in the H<sub>2</sub>-GAC group compared to the H<sub>2</sub>-CON group, with a 46.1 % decrease (Fig. 3c), suggesting that long-term GAC exposure may accelerate microbial activation under high HPP stress. Similar stimulatory effects of carbon materials on the lag phase reduction during AD have been reported. For example, biochar and activated carbon amendments have been shown to enhance microbial activation and shorten lag phases across a variety of substrates, likely due to strengthened microbial interactions and improved extracellular electron transfer (EET) [40–42].

Previous studies have shown that the addition of CMs can enhance the adaptive capacity of anaerobic digesters to environmental stresses, such as high temperature and elevated HPP [43,44]. In this study, short-term GAC supplementation further promoted methanogenic propionate degradation under high HPP stress in sludges from both UASB<sub>CON</sub> and UASB<sub>GAC</sub> reactors. Propionate degradation rates and  $R_{max}$  increased by 46.4 % and 49.8 % in the H<sub>2</sub>-CON<sub>+GAC</sub> group, and by 71.8 % and 90.8 % in the H<sub>2</sub>-GAC<sub>+GAC</sub> group, respectively, compared with their un-supplemented controls. These results suggest that short-term GAC addition may facilitate EET, thereby enhancing propionate degradation. Lag phases were slightly extended in H<sub>2</sub>-CON<sub>+GAC</sub> (3.6 h) and H<sub>2</sub>-GAC<sub>+GAC</sub> (2.9 h) groups likely due to transient disruption of microbe-substrate contact caused by fresh GAC addition, which may temporarily restrict mass transfer and delay microbial adaptation under stress [45]. Notably, the stimulatory effect was more pronounced in sludge previously acclimated to GAC, with degradation rates and  $R_{max}$  increased by 16.2 % and 33.9 % in H<sub>2</sub>-GAC<sub>+GAC</sub> compared with H<sub>2</sub>-CON<sub>+GAC</sub>, accompanied by a 19.3 % reduction in the lag phase. These findings highlight the importance of long-term GAC-induced microbial acclimation in promoting propionate degradation under environmental stress.

#### 3.2.3. GAC effects under stress versus non-stress conditions

As shown in Figs. S1 and S2, high HPP (Section 3.2.2) severely inhibited propionate methanogenesis compared with the N<sub>2</sub>-purged headspace (Section 3.2.1). Propionate degradation rates and  $R_{max}$  decreased by 34.7–42.5 % and 31.6–35.9 %, respectively, in the H<sub>2</sub>-CON and H<sub>2</sub>-GAC groups relative to the N<sub>2</sub>-purged treatments. However, the inhibitory effect was alleviated by short-term GAC amendment, where the reductions in degradation rates and  $R_{max}$  were limited to 6.4–18.9 % and 4.5–9.4 % in H<sub>2</sub>-CON<sub>+GAC</sub> and H<sub>2</sub>-GAC<sub>+GAC</sub>, respectively.

Notably, negligible benefits of short-term GAC addition were observed in sludge from the UASB<sub>CON</sub> reactor under N<sub>2</sub>-purged headspace. The contrasting responses under N<sub>2</sub>-purged and high HPP conditions may arise from different operational conditions. Under the high HPP condition, thermodynamic stress was likely imposed on syntrophic propionate metabolism. GAC supplementation has been shown to promote anaerobic degradation of sludge, potentially by enhancing DIET and mitigating oxidative stress [46]. In this scenario, short-term GAC

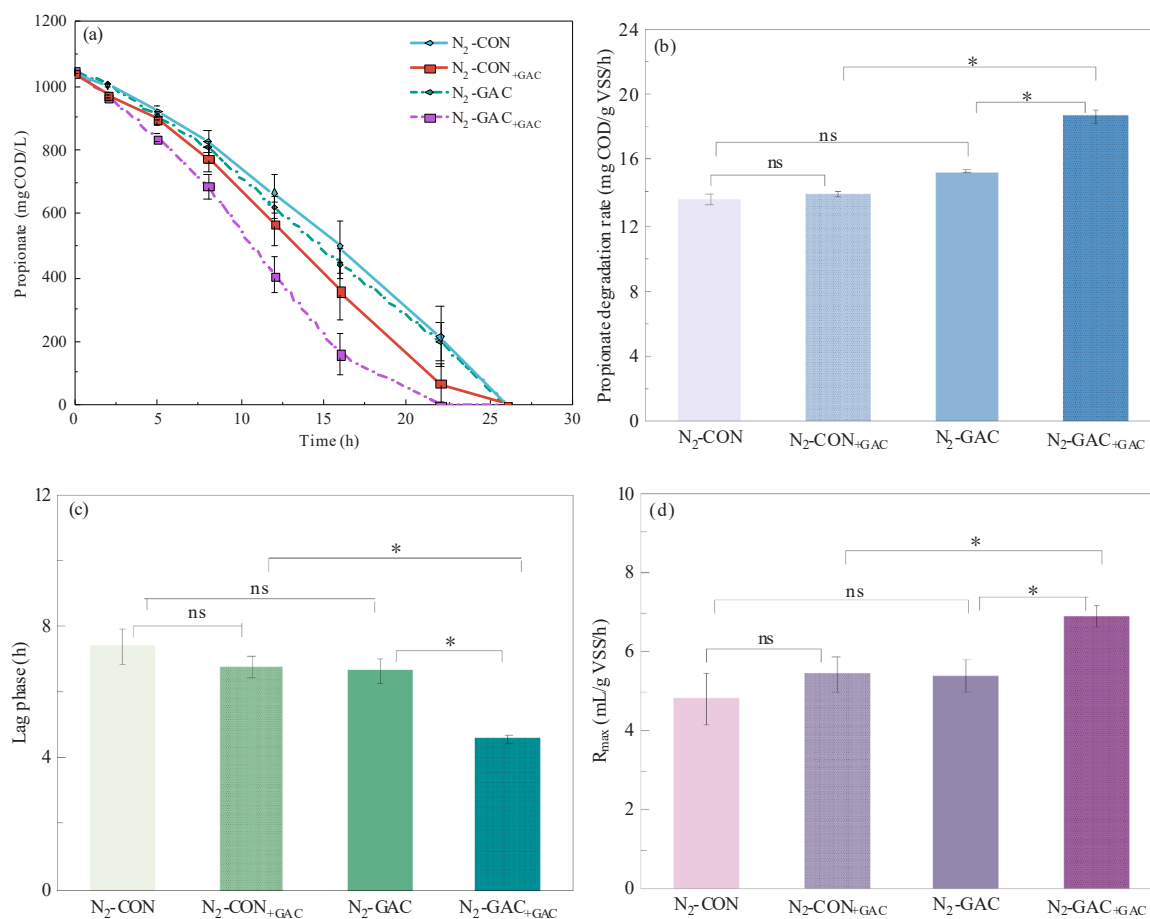


**Fig. 2.** Effects of short-term GAC addition on propionate degradation: (a) Propionate concentration dynamics; (b) Propionate degradation rate; (c) Lag phase; (d) Maximum methane production rate ( $R_{max}$ ) among the four treatment groups. The groups N<sub>2</sub>-CON and N<sub>2</sub>-GAC represent sludge from UASB<sub>CON</sub> and UASB<sub>GAC</sub> reactors, respectively. N<sub>2</sub>-CON+GAC and N<sub>2</sub>-GAC+GAC indicate the corresponding sludge subjected to short-term GAC supplementation during the activity assays. Asterisks (\*) indicate statistically significant differences ( $p < 0.05$ ); “ns” denotes no significant difference ( $p \geq 0.05$ ).

supplementation may enhance propionate degradation through mechanisms in addition to DIET, potentially including mitigation of oxidative stress.

Taken together, these results suggest that GAC has the potential to enhance propionate degradation under stressed conditions, including high OLR and HPP stress. Long-term GAC exposure appears to enrich microbial consortia with enhanced syntrophic capacity. In addition, GAC may additionally promote resilience through stress-mitigation mechanisms. Overall, these findings highlight that GAC stimulates propionate degradation via complementary mechanisms involving microbial adaptation, conductive electron transfer, and possible stress mitigation. Nevertheless, these mechanistic interpretations remain speculative and warrant further validation through microbial community profiling and functional gene analysis.

### 3.3. Microbial responses to increasing OLRs

In response to environmental stress, microbial communities often undergo compositional and functional shifts that enhance anaerobic system stability and resilience [47,48]. GAC has been suggested to modulate microbial community structure and promote functional resilience under stress conditions [49,50]. To examine the role of GAC in microbial dynamics, microbial community composition and metabolic pathways are analyzed in the following section.

#### 3.3.1. Diversity and phylum-level community changes

Alpha-diversity analysis indicated that community richness peaked

at Phase II, with slightly higher Chao1 values in the UASB<sub>GAC</sub> reactor at 267 compared with 240 in the UASB<sub>CON</sub> reactor (Table 2). Although richness declined to 218 in the UASB<sub>CON</sub> reactor by Phase IV, it recovered slightly to 241 in the UASB<sub>GAC</sub> reactor. These findings suggest that excessive OLR suppresses microbial richness in anaerobic systems [51, 52]. Similarly, Khafipour et al. [53] reported that elevating the OLR from 2.8 to 6.1 g COD/L/d, induced by propionic acid addition, led to a decline in microbial diversity in a manure digester. However, GAC supplementation can alleviate such inhibition, thus enhancing system resilience and stability [54–56]. Additionally, Beta diversity analysis showed that the first principal coordinate (PCoA1) explained 49.9 % of the variation (Fig. S3), implying that OLR could be an important driver of community succession.

At the phylum level (Fig. 4a), Halobacterota, Euryarchaeota, and Firmicutes dominated in both systems. Halobacterota, which includes anaerobic methanogens, increased from 24.5 % in the inoculum to over 30 % in two UASB reactors under 7 g COD/L/d, indicating adaptation to elevated OLRs [57,58]. Euryarchaeota encompass diverse methanogens responsible for acetate and hydrogen scavenging [13,59]. Their relative abundance was higher in UASB<sub>GAC</sub> (up to 15.6 %) than in UASB<sub>CON</sub> during Phases I–III, but this trend reversed in Phase IV (16.2 % vs. 11.6 %), reflecting a dynamic response to operational conditions. Firmicutes, involved in hydrolysis and acidogenesis, declined substantially with increasing OLRs, from 15.5 % to 4.2 % in UASB<sub>CON</sub> and from 13.8 % to 5.4 % in UASB<sub>GAC</sub> [60]. Overall, these results suggest that the microbial community structure in the two UASB reactors changed dynamically during the operation.

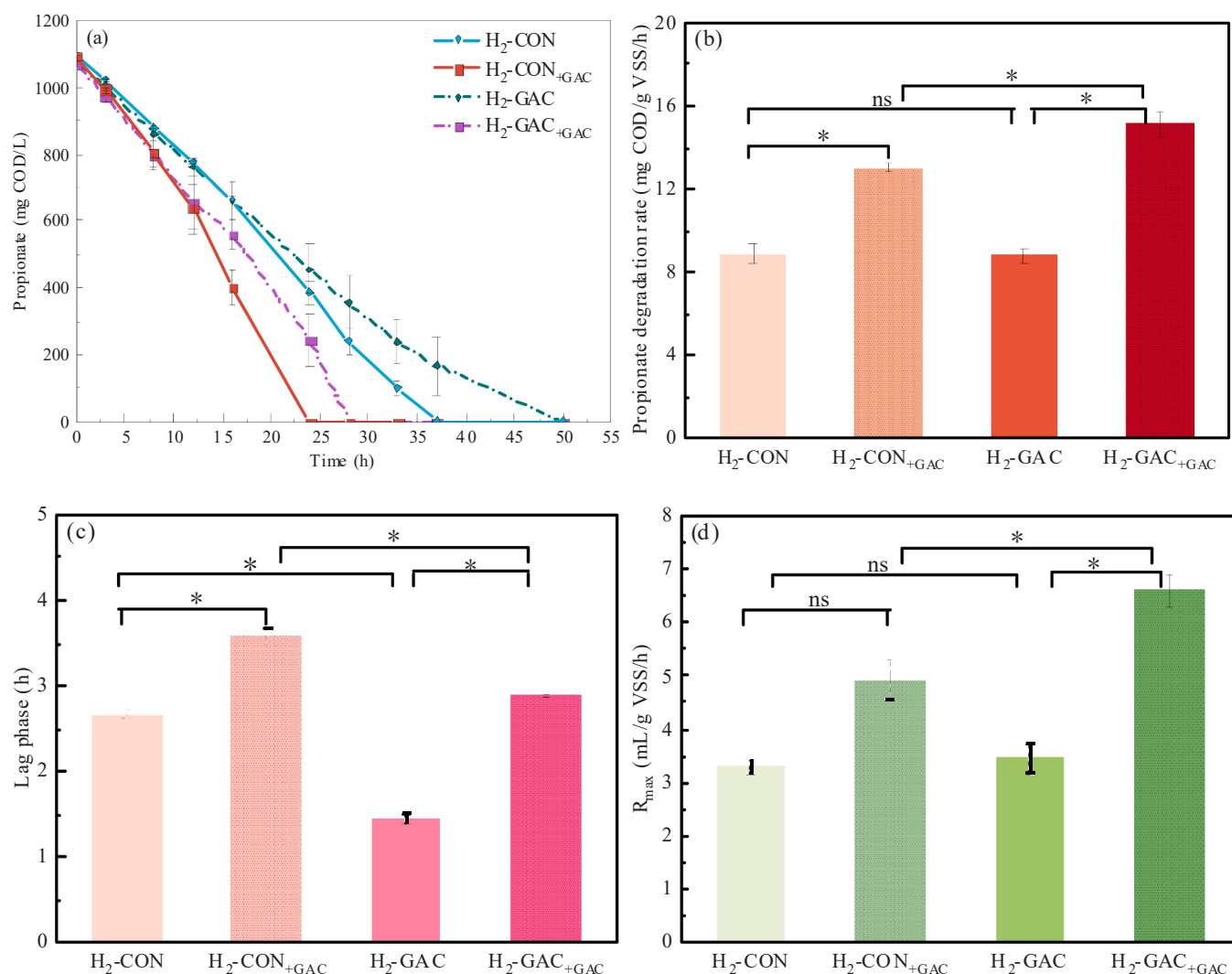


**Fig. 3.** GAC-enhanced propionate degradation under high HPP: (a) Propionate concentration dynamics; (b) Propionate degradation rate; (c) Lag phase; (d)  $R_{max}$  among the four treatment groups. The groups H<sub>2</sub>-CON and H<sub>2</sub>-GAC represent sludge from UASB<sub>CON</sub> and UASB<sub>GAC</sub> reactors, respectively. H<sub>2</sub>-CON+GAC and H<sub>2</sub>-GAC+GAC indicate the corresponding sludge subjected to short-term GAC supplementation during the activity assays. Asterisks (\*) indicate statistically significant differences ( $p < 0.05$ ); “ns” denotes no significant difference ( $p \geq 0.05$ ).

**Table 2**

Alpha diversity indices of microbial communities across operational phases in UASB<sub>CON</sub> and UASB<sub>GAC</sub> reactors.

Reactors	Phases	Alpha diversity index		
		Chao1	Shannon_2	Simpson
UASB <sub>CON</sub>	I	220	3.96	0.13
	II	240	4.19	0.12
	III	231	4.17	0.13
	IV	218	4.04	0.16
UASB <sub>GAC</sub>	I	221	4.00	0.14
	II	267	4.74	0.09
	III	203	3.95	0.15
	IV	241	4.44	0.13

### 3.3.2. Dynamics of syntrophic propionate-oxidizing bacteria (SPOB)

At the genus level, key SPOB including *Syntrophobacter* and *Smithella* [61], showed distinct responses to increasing OLR and GAC supplementation. As shown in Fig. 4b, the relative abundance of *Syntrophobacter* decreased from 9.8 % to 3.7 % in the UASB<sub>CON</sub> reactor and from 7.5 % to 3.2 % in the UASB<sub>GAC</sub> reactor with increasing OLRs, suggesting its sensitivity to substrate overloading. This aligns with previous

observations of *Syntrophobacter* suppression under high OLRs [62].

In contrast, *Smithella* increased from 0.3 % in the seed sludge to 3.2 % and 2.6 % in UASB<sub>CON</sub> and UASB<sub>GAC</sub> reactors, respectively, at Phase IV, indicating their greater tolerance to high OLR conditions (Fig. S4a). Due to its tolerance, *Smithella* likely plays a central role in propionate syntrophic degradation under overloading conditions. The dismutation pathway harbored by *Smithella* provides a thermodynamic advantage over the traditional methylmalonyl-CoA (MMC) pathway [63], which may contribute to its advantage under high OLR. Notably, *Smithella* showed consistently higher levels in the UASB<sub>GAC</sub> reactor during Phases I–III (14.4–82.9 % increase), implying that GAC facilitates its enrichment under moderate loading. *Smithella* has been reported to engage in DIET in the presence of CMs, potentially enhancing its ecological competitiveness and contributing to improved system performance [20,64]. Taken together, these observations suggest that GAC may stimulate DIET between *Smithella* and its syntrophic partners, contributing to stable propionate degradation under high OLRs, consistent with Zhang et al. [65].

Propionate degradation occurs via multiple pathways, including MMC, lactate, hydroxypropionyl, and dismutation routes [66]. The MMC pathway is employed by most known SPOB such as *Syntrophobacter* and *Pelotomaculum*, whereas *Smithella* is the only genus reported

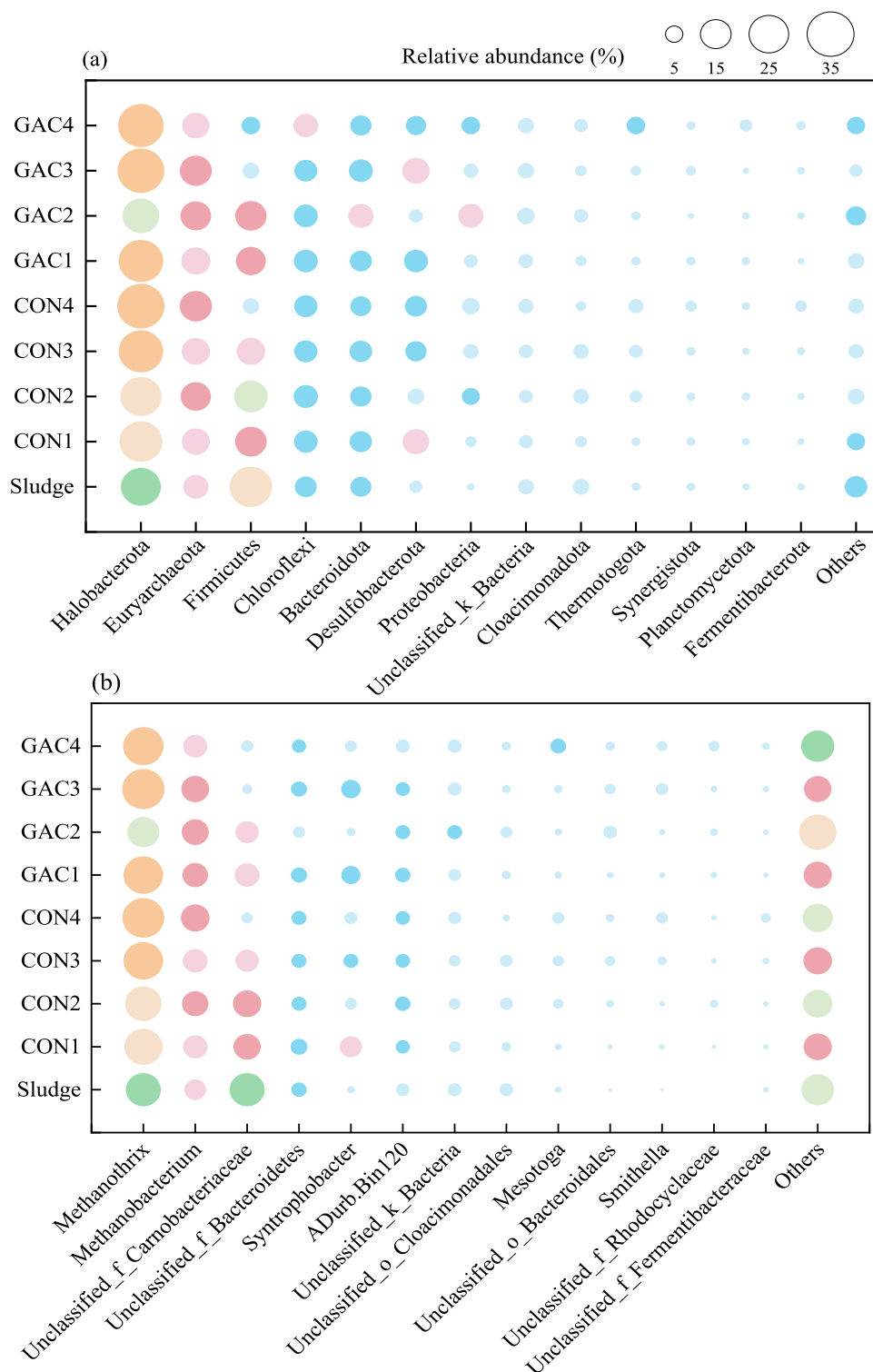


**Fig. 4.** Microbial community composition at the (a) phylum and (b) genus levels in UASB<sub>CON</sub> and UASB<sub>GAC</sub> reactors at the end of Phases I–IV. “Sludge” represents the inoculum. CON1 to CON4 and GAC1 to GAC4 indicate samples collected at the end of each phase. Only taxa with relative abundances > 1 % are shown.

to utilize the dismutation pathway [63,67]. The metabolic pathways and key enzymes involved in propionate-to-methane conversion were reconstructed based on previous studies [68,69], as shown in Fig. 5. In this study, *Syntrophobacter* and *Smithella* dominated both reactors, indicating the coexistence of MMC and dismutation pathways mediated by these taxa, respectively. Enzymes involved in the MMC pathway—EC:2.7.2.15, EC:6.2.1.17, EC:2.8.3.1, EC:6.4.1.3, EC:1.1.5.4, EC:1.1.1.82 and EC:1.8.1.4—were highly enriched in the UASB<sub>GAC</sub>

reactor at Phase II, with EC:1.8.1.4 reaching the highest relative abundance (0.19 %, Table S2). Although their relative abundances decreased with increasing OLRs, the UASB<sub>GAC</sub> reactor consistently maintained values 1.0–5.3 times those in the UASB<sub>CON</sub> reactor at Phase IV.

In the dismutation pathway, propionate is initially converted into acetate and butyrate, with butyrate subsequently degraded via  $\beta$ -oxidation [63]. As shown in Fig. 5, GAC supplementation slightly increased the relative abundances of these genes. In Phase IV, the

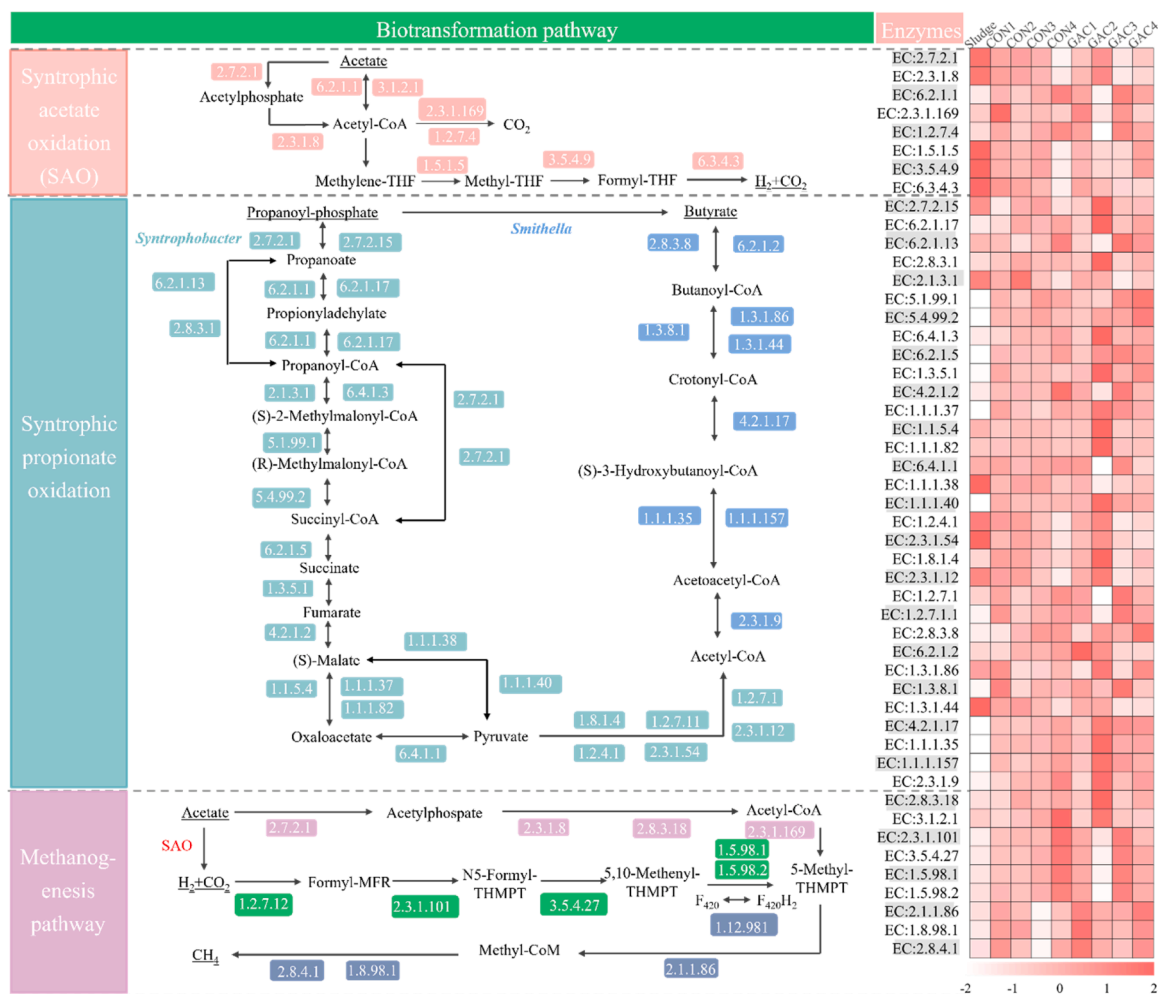


**Fig. 5.** Key metabolic pathways and associated functional enzymes involved in acetate oxidation, propionate oxidation, and methanogenesis in sludge from UASB<sub>CON</sub> and UASB<sub>GAC</sub> reactors at the end of each phase. CON1 to CON4 and GAC1 to GAC4 indicate samples collected at the end of each phase. Relative enzyme abundances (Z-score normalized) are shown by color intensity.

relative abundances of EC:2.8.3.8 and EC:1.3.1.86 were 25.3 % and 63.8 % higher, respectively, in the UASB<sub>GAC</sub> reactor than in the UASB<sub>CON</sub> reactor (Table S2). These results suggest that GAC may enhance the dismutation pathway, consistent with previous reports showing that CMs (e.g., magnetite and carbon nanotubes) promote this pathway through the enrichment of *Smithella* [64]. Additionally, dismutation offers thermodynamic advantages under environmental stress [66,70,71] and has been observed as the dominant propionate oxidation route at 20°C, accompanied by Smithellaceae enrichment and upregulation of functional genes [72]. Consequently, the dismutation pathway stimulated by GAC may provide both metabolic and stability benefits under stressed conditions in anaerobic propionate degradation.

### 3.3.3. Dynamics of syntrophic acetate-oxidizing bacteria (SAOB)

SAOB is critical in syntrophic propionate degradation by consuming acetate intermediates, thereby relieving thermodynamic constraints. *Mesotoga* has recently been identified as a putative SAOB enriched in anaerobic systems [69,73,74]. As shown in Fig. 4b, the relative abundance of *Mesotoga* increased steadily with increasing OLRs, reaching 5.1 % in the UASB<sub>GAC</sub> reactor at Phase IV, which represents a 53.3 % increase relative to the UASB<sub>CON</sub> reactor. This trend is consistent with Zhou et al. [75], who reported that nano-zero-valent iron could stimulate *Mesotoga* growth during anaerobic treatment of antibiotic-containing wastewater. Notably, *Mesotoga* has been classified as an electro-syntrophic microorganism capable of EET [76,77] and may

potentially participate in DIET within methanogenic systems [78]. Consequently, these results suggest that GAC promotes the enrichment of electro-syntrophic taxa, potentially enhancing DIET-mediated interactions in the UASB<sub>GAC</sub> reactor.

As shown in Fig. 5, EC:2.7.2.1 and EC:2.3.1.8, which are shared by both syntrophic acetate oxidation and acetoclastic methanogenesis, were enriched by 18.1 % and 8.6 %, respectively, in the UASB<sub>GAC</sub> reactor compared with the UASB<sub>CON</sub> reactor at Phase IV (Table S3). For SAOB, additional key genes, including EC:1.5.1.5 and EC:6.3.4.3, exhibited a 6.9–16.1 % higher relative abundance in the UASB<sub>GAC</sub> reactor compared to the UASB<sub>CON</sub> reactor, suggesting that GAC addition may enhance SAOB activity under high OLR stress. Such an improvement aligns with previous reports. Pinela et al. [79] showed that iron oxide supplementation increased SAOB relative abundance and activity, facilitating propionate-to-methane conversion under high-ammonia stress. Similarly, Huang et al. [80] demonstrated that the co-addition of GAC and hydrogen stimulated the syntrophic acetate oxidation, thereby enhancing the anaerobic degradation of phenolic wastewater under hypersaline stress.

### 3.3.4. Dynamics of methanogenic archaea

The acetoclastic methanogen *Methanotherix* (formerly *Methanosaeta*) became the dominant archaeal genus in both reactors as OLR increased (Fig. 4b). Its relative abundance increased from 24.0 % in the seed sludge to 34.2 % and 31.7 % in the UASB<sub>CON</sub> and UASB<sub>GAC</sub> reactors,

respectively, at Phase IV. This dominance reflects its tolerance to elevated substrate concentrations [81]. However, the hydrogenotrophic methanogen *Methanobacterium* maintained a stable relative abundance throughout the operation, with ranges of 12.0–16.1 % in the UASB<sub>CON</sub> reactor and 11.6–15.6 % in the UASB<sub>GAC</sub> reactor (Fig. S4b). This stability highlights its resilient hydrogen-scavenging function under elevated OLRs, supporting syntrophic propionate oxidation by maintaining favorable thermodynamics.

Regarding methanogenesis, EC:2.7.2.1 and EC:2.3.1.8 are key enzymes in the conversion of acetate to acetyl-CoA, and their enrichment in the UASB<sub>GAC</sub> reactor further indicates that GAC stimulated the acetate consumption under high OLR conditions. Conversely, hydrogenotrophic methanogenesis-related genes—including EC:2.3.1.101, EC:3.5.4.27, EC:1.5.98.1 and EC:1.5.98.2—were 11.0–18.2 % more abundant in the UASB<sub>CON</sub> reactor than in the UASB<sub>GAC</sub> reactor (Table S4). Although previous studies have reported that GAC can enhance *Methanotherix*-mediated pathway by increasing the abundance of *mer* (EC:1.5.98.2)

and *mtd* (EC:1.5.98.2) genes [18,38], this effect was not evident in the present study. Therefore, the effects of GAC on acetoclastic and hydrogenotrophic methanogenic pathways during propionate degradation warrant further elucidation through metagenomic or metatranscriptomic analyses.

### 3.4. Microbial functional responses to oxidative and electron transfer stressors

High concentrations of propionate can disrupt intracellular homeostasis and impair metabolic cooperation, imposing oxidative stress on microbes [6,82,83]. As shown in Fig. 6, genes associated with both ROS generation (e.g., *mdh* and *adh*) and ROS detoxification (e.g., *gpx1*, *ahpF*, *grxA*, and *oxyR*) were analyzed to assess oxidative stress responses in both reactors [6,20,72]. The relative abundance of *mdh* remained stable (~0.035 %) across all operational phases in both reactors, whereas *adh* gradually increased with increasing OLRs, particularly in the UASB<sub>CON</sub>

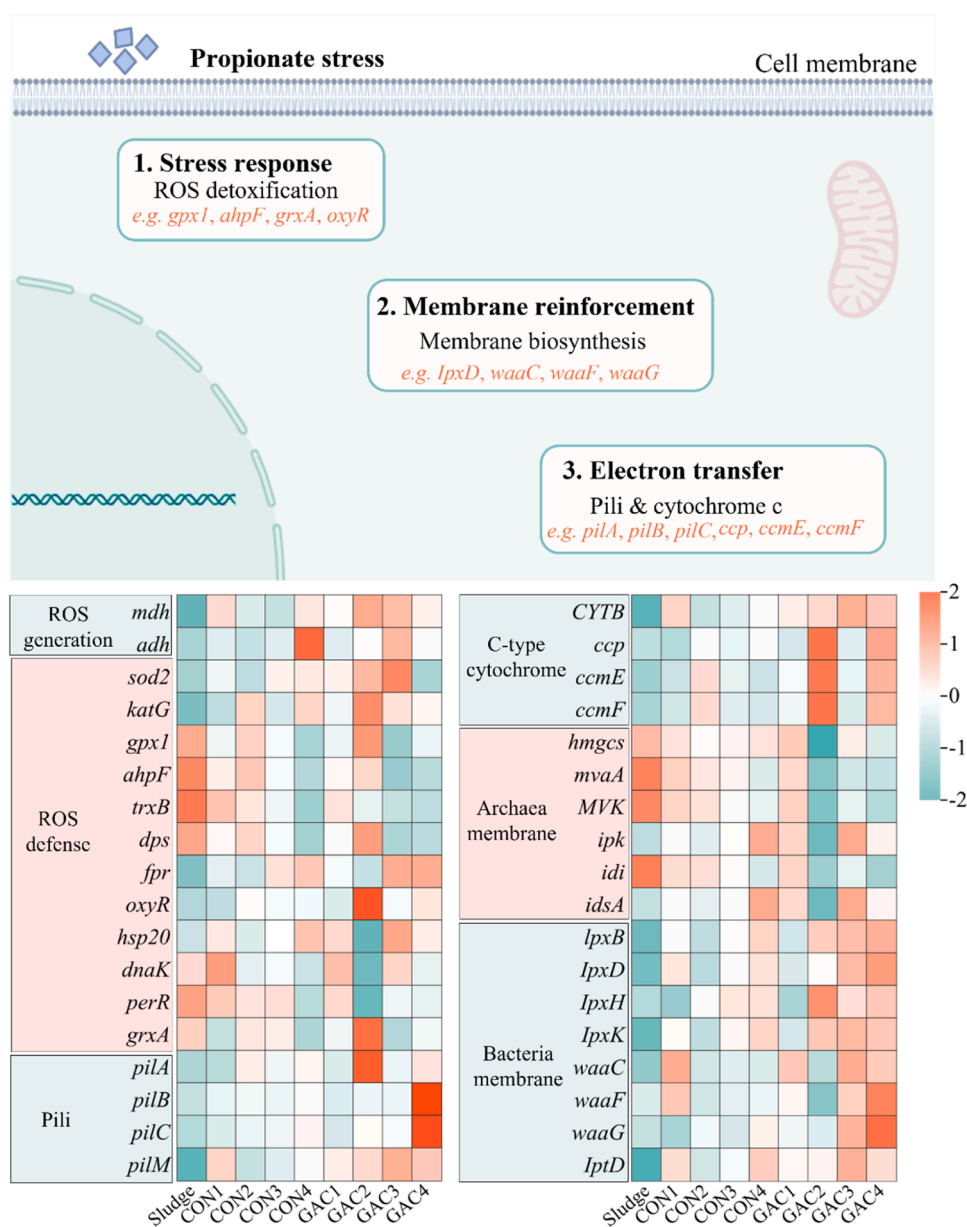


**Fig. 6.** Microbial response to propionate stress based on the Z-score normalized abundance of genes associated with ROS generation and defense, pili formation, cytochrome c maturation, and membrane biosynthesis in bacteria and archaea in UASB<sub>CON</sub> and UASB<sub>GAC</sub> reactors. CON1 to CON4 and GAC1 to GAC4 indicate samples collected at the end of each phase.

reactor (Table S5). Similar upregulation of ROS-associated genes under environmental stressors, such as microplastic exposure, acetate accumulation, and overloading, has been reported [7,84], supporting a link between stress and oxidative responses. During Phase IV, *adh* reached approximately 0.0097 % in the UASB<sub>CON</sub> reactor—1.3 times higher than that in the UASB<sub>GAC</sub> reactor—suggesting elevated oxidative stress without GAC supplementation. In contrast, GAC addition increased the abundances of ROS detoxification genes by 10.1–101.0 % compared with the UASB<sub>CON</sub> reactor at Phase IV. Notably, *oxyR* showed a 119.4 % increase in Phase II in the UASB<sub>GAC</sub> reactor compared with the UASB<sub>CON</sub> reactor. Consistently, the coenzyme F<sub>420</sub> level, involved in ROS reduction [85,86], was 8.3 % higher in the UASB<sub>GAC</sub> reactor than in the UASB<sub>CON</sub> reactor (Fig. S5). These results indicate that GAC could both suppress ROS production and strengthen microbial antioxidant defenses under environmental stress.

Beyond oxidative stress, cell membrane integrity is also critical for microbial survival and function under variable environmental conditions [87]. Environmental stress can alter membrane architecture, modify lipid composition, and compromise viability [88]. As illustrated in Fig. 6, membrane biosynthesis genes exhibited distinct responses between bacteria and archaea in the two reactors. In the UASB<sub>GAC</sub> reactor, genes related to bacterial outer membrane formation (*lpxD*, *waaC*, *waaF*, and *waaG*) were highly increased under high OLR conditions. Their relative abundances ranged from 0.0055 % to 0.035 % during Phase IV, reflecting 8.6–42.9 % increases in the UASB<sub>GAC</sub> reactor compared with the UASB<sub>CON</sub> reactor. This may reflect an adaptive mechanism to enhance membrane integrity and mechanical stability under environmental stress. Conversely, archaeal membrane biosynthesis genes (*hmgcs*, *MVK*, *ipk*, and *idsA*) showed moderate enrichment in the UASB<sub>CON</sub> reactor, with abundances 7.6–10.0 % higher than those in the UASB<sub>GAC</sub> reactor at Phase IV. This suggests that GAC may selectively promote bacterial membrane resilience rather than archaeal membrane remodeling.

Additionally, under high OLR conditions, the UASB<sub>GAC</sub> reactor exhibited notable enrichment of EET-associated genes, including those encoding conductive pili (*pilA*, *pilB*, *pilC*, and *pilM*) and cytochrome c maturation proteins (*CYTB*, *ccp*, *ccmE*, and *ccmF*) [89]. At Phase IV, *pilA*, *pilB*, *pilC*, and *pilM* reached 0.0049 %, 0.043 %, 0.040 %, and 0.015 %, respectively, in the UASB<sub>GAC</sub> reactor, corresponding to 14.3–41.0 % increases over the UASB<sub>CON</sub> reactor. In parallel, the relative abundances of *CYTB*, *ccp*, *ccmE*, and *ccmF* increased by 14.3 %, 65.8 %, 39.2 %, and 34.2 %, respectively, in the UASB<sub>GAC</sub> reactor compared with the UASB<sub>CON</sub> reactor. The consistent upregulation of these EET-associated genes, together with the enrichment of electroactive microbial populations, may support the involvement of DIET-mediated syntrophic propionate oxidation in the UASB<sub>GAC</sub> reactor.

### 3.5. Implications and perspectives

In full-scale anaerobic digesters, feedstock variability and shock loading frequently induce propionate accumulation, undermining process stability and methane productivity [20]. This study demonstrates that GAC supplementation improves system performance and biogas yield under such environmental stresses, possibly by mitigating oxidative stress, reinforcing bacterial membranes, and promoting DIET. These findings underscore its potential as a viable additive for process stabilization in practical applications.

Despite these promising outcomes, several key challenges remain for large-scale deployment. In particular, the relatively high GAC dosage could pose economic constraints for industrial applications. Therefore, optimizing GAC dosing, retention, and recovery is crucial to enhance cost-effectiveness and ensure practical feasibility [44]. Economic assessments considering material costs, GAC lifespan, and potential for regeneration are necessary to guide industrial-scale implementation. Additionally, elucidating the respective contributions of MMC and dismutation pathways is critical for refining operational strategies and

guiding GAC dosing under different loading scenarios. Identifying keystone microbial taxa that underpin GAC-driven process stability will further provide mechanistic insights for the selective enrichment of electroactive and syntrophic propionate-oxidizing populations.

Future research integrating multi-omics approaches (metagenomics, metatranscriptomics, and metabolomics) with reactor-scale engineering trials is warranted to develop scalable and economically viable GAC application protocols. In addition, exploring the interactions between GAC, microbial consortia, and reactor hydrodynamics will inform targeted interventions for enhancing microbial resilience under dynamic and stressed conditions.

## 4. Conclusion

This study suggests that GAC supplementation can enhance methane yield (7.4 % increase) and propionate degradation efficiency (94.6 % vs. 81.4 %) at the OLR of 7 g COD/L/d. With increasing OLRs, GAC mitigated microbial diversity loss (Chao1: 241 in UASB<sub>GAC</sub> vs. 218 in UASB<sub>CON</sub>), and enhanced the relative abundance of *Smithella* by 14.4–82.9 % during Phases I–III and *Mesotoga* by 53.3 % at Phase IV comparing to UASB<sub>CON</sub>. Mechanistically, GAC potentially (i) stimulated propionate degradation and acetate conversion, (ii) alleviated oxidative stress while reinforcing bacterial membrane resilience, and (iii) promoted DIET via upregulation of EET genes. Collectively, these effects improved propionate removal and system resilience, providing mechanistic insights for the practical application of GAC to enhance stable performance under dynamic or stressed conditions.

### CRedit authorship contribution statement

**Wenlong Wang:** Writing – review & editing, Methodology. **Qianyuan Wu:** Writing – review & editing, Methodology. **Huanhuan Chang:** Writing – review & editing, Methodology, Formal analysis. **Chuanqi Liu:** Writing – review & editing, Methodology, Formal analysis. **Guangxue Wu:** Writing – review & editing, Supervision, Project administration, Funding acquisition, Conceptualization. **Tingxia Liu:** Writing – original draft, Methodology, Investigation, Formal analysis, Data curation.

### Declaration of Competing Interest

The authors declare the following financial interests/personal relationships which may be considered as potential competing interests: Guangxue Wu reports financial support was provided by Sustainable Energy Authority of Ireland. Tingxia Liu reports financial support was provided by China Scholarship Council. Guangxue Wu reports financial support was provided by Galway University Foundation CLG.

### Acknowledgements

This research was supported by the Sustainable Energy Authority of Ireland (SEAI; 21/RDD/600). Tingxia Liu thanks the scholarship from China Scholarship Council (No: 202206690019). Guangxue Wu thanks the support from Galway University Foundation.

### Appendix A. Supporting information

Supplementary data associated with this article can be found in the online version at [doi:10.1016/j.jece.2026.121343](https://doi.org/10.1016/j.jece.2026.121343).

### Data availability

Data will be made available on request.

## References

- [1] Y. Ma, L. Li, P. Yang, Y. Peng, X. Peng, Exploring instability mechanisms of overloaded anaerobic digestion based on the combination of degradation dynamics of acetate and propionate and metagenomics assay, *Biochem. Eng. J.* 198 (2023) 109032.
- [2] L. Regueiro, J.M. Lema, M. Carballa, Key microbial communities steering the functioning of anaerobic digesters during hydraulic and organic overloading shocks, *Bioresour. Technol.* 197 (2015) 208–216.
- [3] P. Rusanowska, M. Zieliński, M. Kisielska, M. Dudek, L. Paukzto, M. Dębowski, Methane production, microbial community, and volatile fatty acids profiling during anaerobic digestion under different organic loading, *Energies* 18 (3) (2025) 575.
- [4] R. Saidi, M. Hamdi, H. Bouallagui, Enhanced hydrogen and methane production from date fruit wastes using semi continuous two-stage anaerobic digestion process with increasing organic loading rates, *Process Saf. Environ. Prot.* 174 (2023) 267–275.
- [5] Y. Jing, J. Wan, I. Angelidaki, S. Zhang, G. Luo, iTRAQ quantitative proteomic analysis reveals the pathways for methanation of propionate facilitated by magnetite, *Water Res.* 108 (2017) 212–221.
- [6] M. Yan, Z. Hu, Z. Duan, Y. Sun, T. Dong, X. Sun, F. Zhen, Y. Li, Microbiome re-assembly boosts anaerobic digestion under volatile fatty acid inhibition: focusing on reactive oxygen species metabolism, *Water Res.* 246 (2023) 120711.
- [7] X. Zhu, E. Blanco, M. Bhatti, A. Borrión, Improving anaerobic digestion process against acetate accumulation: insights into organic loading rates and nano magnetite additions, *Chem. Eng. J.* 512 (2025) 162641.
- [8] R.M. Alonso, A. Escapa, A. Sotres, A. Moran, Integrating microbial electrochemical technologies with anaerobic digestion to accelerate propionate degradation, *Fuel* 267 (2020) 117158.
- [9] B. Suraraks, N. Hudayah, N. Boonapatcharoen, V. Kongduan, D. Phalaphol, W. Suksong, K. Kusonmano, M. Tanticharoen, K. Kuroda, T. Yamaguchi, Establishment of syntrophic methanogenic consortia (SMC) in different sludges from various full-scale biogas plants using sodium propionate, *J. Environ. Chem. Eng.* 13 (2) (2025) 115863.
- [10] P.C. Pullammanappallil, D.P. Chynoweth, G. Lyberatos, S.A. Svoronos, Stable performance of anaerobic digestion in the presence of a high concentration of propionic acid, *Bioresour. Technol.* 78 (2) (2001) 165–169.
- [11] Y. Han, H. Green, W. Tao, Reversibility of propionic acid inhibition to anaerobic digestion: inhibition kinetics and microbial mechanism, *Chemosphere* 255 (2020) 126840.
- [12] P.S. Calabrò, F. Fazzino, C. Limonti, A. Siciliano, Enhancement of anaerobic digestion of waste-activated sludge by conductive materials under high volatile fatty acids-to-alkalinity ratios, *Water* 13 (4) (2021) 391.
- [13] Y. Lei, D. Sun, Y. Dang, X. Feng, D. Huo, C. Liu, K. Zheng, D.E. Holmes, Metagenomic analysis reveals that activated carbon aids anaerobic digestion of raw incineration leachate by promoting direct interspecies electron transfer, *Water Res.* 161 (2019) 570–580.
- [14] Y. Li, N. Lv, F. Zhong, X. Pan, G. Zhu, Enhancing anaerobic digestion through nanoscale zero-valent iron, multi-walled carbon nanotubes, and graphene family materials: Mitigating formate stress inhibition in syntrophic propionate metabolism, *J. Water Process Eng.* 79 (2025) 109034.
- [15] F. Liu, A.E. Rotaru, P.M. Shrestha, N.S. Malvankar, K.P. Nevin, D.R. Lovley, Promoting direct interspecies electron transfer with activated carbon, *Energy Environ. Sci.* 5 (10) (2012) 8982–8989.
- [16] A. Mou, N. Yu, X. Yang, Y. Liu, Enhancing methane production in up-flow Anaerobic sludge blanket (UASB) reactors: influence of solid content on granular activated carbon (GAC) biofilm community dynamics, *ACS EST Eng.* 5 (10) (2025) 2532–2542.
- [17] C. Bais, Y. Zhang, Q. Huang, C. Benally, Y. Liu, Granular activated carbon enhances microbial activity in anaerobic reactors: Insights from metagenomics and metaproteomics, *Biochem. Eng. J.* (2025) 109843.
- [18] H. He, Y. Zeng, H. Dong, P. Cui, W. Lu, H. Xu, B. Qiu, D. Sun, J. Ma, Y. Dang, Enrichment of *Methanoxystrix* species via riboflavin-loaded granular activated carbon in anaerobic digestion of high-concentration brewery wastewater amidst continuous inoculation of *Methanosarcina barkeri*, *Water Res.* 268 (2025) 122739.
- [19] H. Dang, N. Yu, A. Mou, L. Zhang, B. Guo, Y. Liu, Metagenomic insights into direct interspecies electron transfer and quorum sensing in blackwater anaerobic digestion reactors supplemented with granular activated carbon, *Bioresour. Technol.* 352 (2022) 127113.
- [20] Y. Su, L. Feng, X. Duan, H. Peng, Y. Zhao, Y. Chen, Deciphering the function of Fe<sub>3</sub>O<sub>4</sub> in alleviating propionate inhibition during high-solids anaerobic digestion: insights of physiological response and energy conservation, *Water Res.* 270 (2025) 122811.
- [21] X. Zhu, E. Blanco, M. Bhatti, A. Borrión, Mitigating overload-induced stress in anaerobic digestion: long-term performance and fate of nano magnetite additives, *Water Res.* (2025) 124241.
- [22] H.H. Fang, Y. Li, H. Chui, Performance and sludge characteristics of UASB process treating propionate-rich wastewater, *Water Res.* 29 (3) (1995) 895–898.
- [23] J. Ma, L.J. Mungoni, W. Verstraete, M. Carballa, Maximum removal rate of propionic acid as a sole carbon source in UASB reactors and the importance of the macro-and micro-nutrients stimulation, *Bioresour. Technol.* 100 (14) (2009) 3477–3482.
- [24] B. Du, X. Zhan, P.N. Lens, Y. Zhang, G. Wu, Deciphering anaerobic ethanol metabolic pathways shaped by operational modes, *Water Res.* 249 (2024) 120896.
- [25] Y. Zhang, L. Zhang, B. Guo, Y. Zhou, M. Gao, A. Sharaf, Y. Liu, Granular activated carbon stimulated microbial physiological changes for enhanced anaerobic digestion of municipal sewage, *Chem. Eng. J.* 400 (2020) 125838.
- [26] Z. Wang, S. Wang, Y. Hu, B. Du, J. Meng, G. Wu, H. Liu, X. Zhan, Distinguishing responses of acetoclastic and hydrogenotrophic methanogens to ammonia stress in mesophilic mixed cultures, *Water Res.* 224 (2022) 119029.
- [27] M.H. Zwietering, I. Jongenburger, F.M. Rombouts, K. Van't Riet, Modeling of the bacterial growth curve, *Appl. Environ. Microbiol.* 56 (6) (1990) 1875–1881.
- [28] APHA, 2005 Standard Methods for the Examination of Water and Wastewater (21st Ed.), American Public Health Association, American Water Works Association, Water Environment Federation, Washington DC.
- [29] G.M. Douglas, V.J. Maffei, J.R. Zaneveld, S.N. Yurgel, J.R. Brown, C.M. Taylor, C. Huttenhower, M.G. Langille, PICRUSt2 for prediction of metagenome functions, *Nat. Biotechnol.* 38 (6) (2020) 685–688.
- [30] S. Chen, A.E. Rotaru, P.M. Shrestha, N.S. Malvankar, F. Liu, W. Fan, K.P. Nevin, D.R. Lovley, Promoting interspecies electron transfer with biochar, *Sci. Rep.* 4 (1) (2014) 5019.
- [31] G. Ren, P. Chen, J. Yu, J. Liu, J. Ye, S. Zhou, Recyclable magnetite-enhanced electromethanogenesis for biomethane production from wastewater, *Water Res.* 166 (2019) 115095.
- [32] P. Zhang, J. Zhang, T. Zhang, L. Zhang, Y. He, Zero-valent iron enhanced methane production of anaerobic digestion by reinforcing microbial electron bifurcation coupled with direct inter-species electron transfer, *Water Res.* 255 (2024) 121428.
- [33] Y. Li, Y. Sun, G. Yang, K. Hu, P. Lv, L. Li, Vertical distribution of microbial community and metabolic pathway in a methanogenic propionate degradation bioreactor, *Bioresour. Technol.* 245 (2017) 1022–1029.
- [34] Y. Dang, D.E. Holmes, Z. Zhao, T.L. Woodard, Y. Zhang, D. Sun, L.Y. Wang, K. P. Nevin, D.R. Lovley, Enhancing anaerobic digestion of complex organic waste with carbon-based conductive materials, *Bioresour. Technol.* 220 (2016) 516–522.
- [35] T.H. Tsui, H. Wu, B. Song, S.S. Liu, A. Bhardwaj, J.W. Wong, Food waste leachate treatment using an Upflow Anaerobic Sludge Bed (UASB): Effect of conductive material dosage under low and high organic loads, *Bioresour. Technol.* 304 (2020) 122738.
- [36] J. Xiao, M. Qaisar, X. Zhu, W. Li, K. Zhang, N. Liang, H. Feng, J. Cai, Conductive materials enhance anaerobic membrane bioreactor (AnMBR) treating waste leachate at high organic loading rates, *J. Environ. Manag.* 375 (2025) 124277.
- [37] G. Giangeri, P. Tsapekos, D. Pitsikoglou, G. Ghiotto, M.K.T.H. Lin, L. Treu, S. Campanaro, I. Angelidaki, Deciphering direct interspecies electron transfer activity in microbial interactions: the influence of conductive materials in anoxic ecosystems, *Chem. Eng. J.* 503 (2025) 158716.
- [38] L. Wang, J. Ma, W. Xing, H. Yao, D. Sun, Y. Dang, Metagenomic insights towards understanding the role of riboflavin-loaded granular activated carbon and *Methanosarcina barkeri* co-addition in enhancing anaerobic digestion, *J. Water Process Eng.* 73 (2025) 107690.
- [39] J. Yang, K. Shen, C. He, L. Xu, H. Shen, C. Xu, Z.H. Hu, W. Wang, Impact of carbon-based conductive materials on performance and microbial community composition during anaerobic digestion of butanol-octanol wastewater, *Bioresour. Technol.* 417 (2025) 131880.
- [40] C. Deng, X. Kang, R. Lin, B. Wu, X. Ning, D. Wall, J.D. Murphy, Boosting biogas production from recalcitrant lignin-based feedstock by adding lignin-derived carbonaceous materials within the anaerobic digestion process, *Energy* 278 (2023) 127819.
- [41] A. Hackula, X. Ning, G. Collins, S.A. Jackson, N.D. O'Leary, C. Deng, R. O'Shea, J.D. Murphy, D.M. Wall, Investigating the effects of whiskey-barrel derived biochar addition to anaerobic digestion at a distillery: a study on energy yield and system efficiency, *Energy Convers. Manag.* X 23 (2024) 100654.
- [42] R. Jia, Q. Tao, D. Sun, Y. Dang, Carbon cloth self-forming dynamic membrane enhances anaerobic removal of organic matter from incineration leachate via direct interspecies electron transfer, *Chem. Eng. J.* 445 (2022) 136732.
- [43] W. Yan, N. Shen, Y. Xiao, Y. Chen, F. Sun, V.K. Tyagi, Y. Zhou, The role of conductive materials in the start-up period of thermophilic anaerobic system, *Bioresour. Technol.* 239 (2017) 336–344.
- [44] X. Zhou, M. Guo, X. Fu, D. Wang, J. Liao, W. Xu, H. Han, Insights into microbial metabolic coordination under driving force of different conductive materials-mediated direct interspecies electron transfer during anaerobic digestion, *Chem. Eng. J.* 496 (2024) 154230.
- [45] Y. Wu, S. Wang, D. Liang, N. Li, Conductive materials in anaerobic digestion: from mechanism to application, *Bioresour. Technol.* 298 (2020) 122403.
- [46] S.M.M. Azizi, B.S. Zakaria, N. Haffiez, B.R. Dhar, Granular activated carbon remediates antibiotic resistance propagation and methanogenic inhibition induced by polystyrene nanoplastics in sludge anaerobic digestion, *Bioresour. Technol.* 377 (2023) 128938.
- [47] S. Wang, Y. Deng, K. Zhang, Z. Jiang, Z. Chen, Y. Miao, K. Huang, C. Hu, Z. Wang, Volatile fatty acids production and sulfur metabolism pathways altered in a two-phase anaerobic sulfate-reducing system due to high organic and sulfate loading rates, *J. Water Process Eng.* 70 (2025) 106948.
- [48] L. Bucci, G. Ghiotto, G. Zampieri, R. Raga, L. Favaro, L. Treu, S. Campanaro, Adaptation of anaerobic digestion microbial communities to high ammonium levels: insights from strain-resolved metagenomics, *Environ. Sci. Technol.* 58 (1) (2023) 580–590.
- [49] W.A. Cavalcante, M. del Pilar Anzola Rojas, C.A. de Menezes, F. Eng, R.C. Leitao, T. A. Gehring, M. Zaiat, Direct interspecies electron transfer stimulated in anaerobic structured-bed reactors under microbial stress conditions, *J. Environ. Chem. Eng.* 12 (6) (2024) 114398.
- [50] D. Johnravindar, B. Liang, R. Fu, G. Luo, H. Meruvu, S. Yang, B. Yuan, Q. Fei, Supplementing granular activated carbon for enhanced methane production in

- anaerobic co-digestion of post-consumer substrates, *Biomass.. Bioenergy* 136 (2020) 105543.
- [51] C.M. Duong, T.T. Lim, Optimization and microbial diversity of anaerobic co-digestion of swine manure with waste kitchen oil at high organic loading rates, *Waste Manag.* 154 (2022) 199–208.
- [52] N. Wongfaed, P. Kongjan, P.O. Prasertsan, S. Thong, Effect of oil and derivative in palm oil mill effluent on the process imbalance of biogas production, *J. Clean. Prod.* 247 (2020) 119110.
- [53] A. Khafipour, E.M. Jordaan, D. Flores Orozco, E. Khafipour, D.B. Levin, R. Sparling, N. Cicek, Response of microbial community to induced failure of anaerobic digesters through overloading with propionic acid followed by process recovery, *Front. Bioeng. Biotechnol.* 8 (2020) 604838.
- [54] P. Jiao, Y. Zhou, X. Zhang, H. Jian, X.X. Zhang, L. Ma, Mechanisms of horizontal gene transfer and viral contribution to the fate of intracellular and extracellular antibiotic resistance genes in anaerobic digestion supplemented with conductive materials under ammonia stress, *Water Res.* 267 (2024) 122549.
- [55] A. Mou, N. Yu, X. Yang, Y. Liu, Enhancing methane production and organic loading capacity from high solid-content wastewater in modified granular activated carbon (GAC)-amended up-flow anaerobic sludge blanket (UASB), *Sci. Total Environ.* 906 (2024) 167609.
- [56] J. Yang, K. Liu, W. Yi, B. Si, C. Tian, G. Yang, Effects of biochar, granular activated carbon, and magnetite on the electron transfer of microbials during the anaerobic digestion process: insights into nitrogen heterocyclic compounds degradation, *Fuel* 358 (2024) 130079.
- [57] J. Martijn, M.E. Schön, A.E. Lind, J. Vosseberg, T.A. Williams, A. Spang, T. J. Ettema, Hikarchaea demonstrate an intermediate stage in the methanogen-to-halophile transition, *Nat. Commun.* 11 (1) (2020) 5490.
- [58] J.R. Ottoni, S.P.F. Bernal, T.J. Marterres, F.N. Luiz, V.P. Dos Santos, Á.G. Mari, J. G. Somer, V.M. de Oliveira, M.R.Z. Passarini, Cultured and uncultured microbial community associated with biogas production in anaerobic digestion processes, *Arch. Microbiol.* 204 (6) (2022) 340.
- [59] S. Xue, Y. Wang, X. Lyu, N. Zhao, J. Song, X. Wang, G. Yang, Interactive effects of carbohydrate, lipid, protein composition and carbon/nitrogen ratio on biogas production of different food wastes, *Bioresour. Technol.* 312 (2020) 123566.
- [60] Y. Zhang, B. Guo, L. Zhang, H. Zhang, Y. Liu, Microbial community dynamics in granular activated carbon enhanced up-flow anaerobic sludge blanket (UASB) treating municipal sewage under sulfate reducing and psychrophilic conditions, *Chem. Eng. J.* 405 (2021) 126957.
- [61] Y. Liu, D.L. Balkwill, H.C. Aldrich, G.R. Drake, D.R. Boone, Characterization of the anaerobic propionate-degrading syntrophs *Smithella propionica* gen. nov., sp. nov. and *Syntrophobacter wolinii*, *Int. J. Syst. Evolut. Microbiol.* 49 (2) (1999) 545–556.
- [62] G. Baek, J. Kim, J. Kim, C. Lee, Individual and combined effects of magnetite addition and external voltage application on anaerobic digestion of dairy wastewater, *Bioresour. Technol.* 297 (2020) 122443.
- [63] F.A. de Bok, A.J. Stams, C. Dijkema, D.R. Boone, Pathway of propionate oxidation by a syntrophic culture of *Smithella propionica* and *Methanospirillum hungatei*, *Appl. Environ. Microbiol.* 67 (4) (2001) 1800–1804.
- [64] X. Xia, J. Zhang, T. Song, Y. Lu, Stimulation of *Smithella*-dominating propionate oxidation in a sediment enrichment by magnetite and carbon nanotubes, *Environ. Microbiol. Rep.* 11 (2) (2019) 236–248.
- [65] Y. Zhang, B. Guo, H. Dang, L. Zhang, H. Sun, N. Yu, Y. Tang, Y. Liu, Roles of granular activated carbon (GAC) and operational factors on active microbiome development in anaerobic reactors, *Bioresour. Technol.* 343 (2022) 126104.
- [66] Y. Jin, Y. Lu, Syntrophic propionate oxidation: one of the rate-limiting steps of organic matter decomposition in anoxic environments, *Appl. Environ. Microbiol.* 89 (5) (2023) e00384–23.
- [67] M. Westerholm, M. Calusinska, J. Dolfing, Syntrophic propionate-oxidizing bacteria in methanogenic systems, *FEMS Microbiol. Rev.* 46 (2) (2022) fuab057.
- [68] Q. Sun, D. Li, Y. He, Q. Ping, L. Wang, Y. Li, Improved anaerobic digestion of waste activated sludge under ammonia stress by nanoscale zero-valent iron/peracetic acid pretreatment and hydrochar regulation: Insights from multi-omics analyses, *Water Res.* 279 (2025) 123497.
- [69] M. Zhang, Y. Han, Y. Zeng, T. Wang, Z. Wang, Y. Wu, N. Li, F.L. Lobo, X. Wang, Understanding the microbial processes on carbon brushes that accelerate methanogenesis of long-chain fatty acids in anaerobic digestion, *Water Res.* 273 (2025) 123084.
- [70] M. Adams, Ammonia-stressed anaerobic digestion: sensitivity dynamics of key syntrophic interactions and methanogenic pathways-A review, *J. Environ. Manag.* 371 (2024) 123183.
- [71] F. De Bok, C. Plugge, A. Stams, Interspecies electron transfer in methanogenic propionate degrading consortia, *Water Res.* 38 (6) (2004) 1368–1375.
- [72] M. Yan, Z. Shi, X. Zhang, X. Lin, Y. Sun, X. Cheng, H. Tian, Y. Li, Decipher syntrophies and adaptive response towards enhancing conversion of propionate to methane under psychrophilic condition, *Water Res.* 274 (2025) 123143.
- [73] J. Du, H. Liang, B. Wen, B. Li, X.Y. Li, L. Lin, Bio-electroreduction of CO<sub>2</sub> to acetate: impact of the inorganic carbon feeding regime on microbial electrosynthesis, *J. Water Process Eng.* 70 (2025) 107108.
- [74] Y. Zeng, X. Zhong, Y. Chen, M. Gou, K. Yu, Y.Q. Tang, Characteristics of phages and their interactions with hosts in anaerobic reactors, *Environ. Microbiol.* 27 (1) (2025) e70040.
- [75] L. Zhou, J. Li, X. Lu, W. Zhang, B. Pan, M. Hua, Simultaneous effects of nanoscale zero-valent iron on wastewater decontamination and energy generation: mechanisms of sulfamethoxazole degradation and methanogenesis, *J. Hazard. Mater.* 481 (2025) 136569.
- [76] Y. Li, S. Wang, R. Dong, X. Li, A large cathode surface area promotes electromethanogenesis at a proper external voltage in a single coaxial microbial electrolysis cell, *Sci. Total Environ.* 868 (2023) 161721.
- [77] G. Baek, J. Kim, C. Lee, Effectiveness of electromagnetic in situ magnetite capture in anaerobic sequencing batch treatment of dairy effluent under electro-syntrophic conditions, *Renew. Energy* 179 (2021) 105–115.
- [78] Y. Li, W. Kong, H. Liu, Y. Hong, T. Huang, Enhanced degradation of phenolic compounds in coal gasification wastewater by activated carbon-Fe<sub>3</sub>O<sub>4</sub> nanoparticles coupled with anaerobic co-metabolism, *Biochem. Eng. J.* 189 (2022) 108717.
- [79] E. Pinela, A. Schnürer, A. Neubeck, J. Moestedt, M. Westerholm, Impact of additives on syntrophic propionate and acetate enrichments under high-ammonia conditions, *Appl. Microbiol. Biotechnol.* 108 (1) (2024) 433.
- [80] Z. Huang, C. He, F. Dong, K. Su, S. Yuan, Z. Hu, W. Wang, Granular activated carbon and exogenous hydrogen enhanced anaerobic digestion of hypersaline phenolic wastewater via syntrophic acetate oxidation and hydrogenotrophic methanogenesis, *Bioresour. Technol.* 365 (2022) 128155.
- [81] M. Gaspari, G. Ghiotto, V.B. Centurion, T. Kotsopoulos, D. Santinello, S. Campanaro, L. Treu, P.G. Kougias, Decoding microbial responses to ammonia shock loads in biogas reactors through metagenomics and metatranscriptomics, *Environ. Sci. Technol.* 58 (1) (2023) 591–602.
- [82] T. Dogan, O. Ince, N.A. Oz, B.K. Ince, Inhibition of volatile fatty acid production in granular sludge from a UASB reactor, *J. Environ. Sci. Health* 40 (3) (2005) 633–644.
- [83] Q. Li, Y. Liu, X. Yang, J. Zhang, B. Lu, R. Chen, Kinetic and thermodynamic effects of temperature on methanogenic degradation of acetate, propionate, butyrate and valerate, *Chem. Eng. J.* 396 (2020) 125366.
- [84] T. Luo, X. Dai, Z. Chen, L. Wu, W. Wei, Q. Xu, B.J. Ni, Different microplastics distinctively enriched the antibiotic resistance genes in anaerobic sludge digestion through shifting specific hosts and promoting horizontal gene flow, *Water Res.* 228 (2023) 119356.
- [85] Q.V. Vo, N.T. Hoa, N.K. Hien, P.C. Nam, D.T. Quang, A. Mechler, Modeling the antioxidant behavior of F<sub>420</sub> coenzyme: a computational study, *N. J. Chem.* 49 (18) (2025) 7426–7434.
- [86] G. Bashiri, Cofactor F<sub>420</sub>, an emerging redox power in biosynthesis of secondary metabolites, *Biochem. Soc. Trans.* 50 (1) (2022) 253–267.
- [87] W.N. Konings, S.V. Albers, S. Koning, A.J. Driessen, The cell membrane plays a crucial role in survival of bacteria and archaea in extreme environments, *Antonie Van Leeuwenhoek* 81 (1) (2002) 61–72.
- [88] V.W. Rowlett, V.K. Mallampalli, A. Karlstaedt, W. Dowhan, H. Taegtmeier, W. Margolin, H. Vitrac, Impact of membrane phospholipid alterations in *Escherichia coli* on cellular function and bacterial stress adaptation, *J. Bacteriol.* 199 (13) (2017) 1100–1128.
- [89] D.W. Ding, J. Xu, L. Li, J.M. Xie, X. Sun, Identifying the potential extracellular electron transfer pathways from ac-type cytochrome network, *Mol. Biosyst.* 10 (12) (2014) 3138–3146.